ELSEVIER

Development of molecular hydrogen-bonding potentials (MHBPs) and their application to structure–permeation relations

Sébastien Rey,* Giulia Caron,† Giuseppe Ermondi,† Patrick Gaillard,* Alessandra Pagliara,* Pierre-Alain Carrupt,* and Bernard Testa*

**Institut de Chimie Thérapeutique, Section de Pharmacie, Université de Lausanne, Lausanne, Switzerland*
†Permanent address: Dipartimento di Scienza e Tecnologia del Farmaco, Università di Torino, Torino, Italy

Hydrogen bonds are major forces of recognition in biochemistry and molecular pharmacology; they are an essential component of intermolecular interactions and determine to a significant extent the 3D-structure of bio-macromolecules. To explore three-dimensional H-bonding properties, a new tool called Molecular Hydrogen-Bonding Potentials (MHBPs) was created. The development of this tool is based on a stepwise procedure similar to the one used successfully to generate the Molecular Lipophilicity Potential (MLP). First, a H-bonding fragmental system was developed starting from published solvatochromic parameters. An atomic H-bonding donor fragmental value (α) is associated to each hydrogen atom in a polar moiety. Similarly, an atomic H-bonding acceptor fragmental value (β) is associated to each polar atom. A distance function and an angle function were defined to take into account variations of the MHBPs in space. The fragmental system and the geometric functions were then combined to generate the MHBPs. These are calculated at each point of an adequate molecular surface or on a three-dimensional grid. The MHBPs were compared with GRID interactions energies and correlated with success to oral drug absorption data. Available examples demonstrate that the MHBPs are a promising computational tool in drug design. Their combination with CoMFA and VolSurf is being studied. © 2001 by Elsevier Science Inc.

Keywords: molecular hydrogen-bonding potentials, MHBPs, quantitative structure–activity relationships; QSAR; oral drug absorption

Color Plates for this article are on pages 594 and 597.

Corresponding author: P.A. Carrupt, Institut de Chimie Thérapeutique, Section de Pharmacie, Université de Lausanne, CH-1015 Lausanne, Switzerland. Fax: +41 21 - 692 45 25.

E-mail address: Pierre-Alain.Carrupt@ict.unil.ch (P.A. Carrupt)

INTRODUCTION

The chemical and biochemical significance of hydrogen bonds, particularly in biological recognition, has been acknowledged since this concept was first formulated at the beginning of the twentieth century. The conformational stabilization of proteins by internal H-bonds and the transfer of protons via H-bonds in enzymes are two telling examples. Further important roles are played by H-bonds in ligand–receptor interactions,[1] permeant-membrane interactions,[2] oral and percutaneous absorption[3–6] and brain penetration.[7,8]

Various methods exist to measure or calculate the H-bonding capacity of solutes. Experimental H-bonding molecular descriptors are the H-bonding donor acidity (α) and the H-bonding acceptor basicity (β). Abraham[9,10] and Raevsky[11] have developed quantitative scales of H-bonding acidity and basicity based on lipophilicity and thermodynamic data. The difference between two different log P scales is another experimental H-bonding descriptor.[12,13] El Tayar and colleagues have developed the Λ descriptor, obtained from experimental lipophilicity data and from calculated molecular volumes, to obtain an indirect estimate of H-bonding properties.[14]

Among theoretical methods to describe molecular H-bonding properties, the counting of the number of groups

Journal of Molecular Graphics and Modelling 19, 521–535, 2001

655 Avenue of the Americas, New York, NY 10010

1093-3263/01/$–see front matter
PII S1093-3263(01)00105-4

able to form H-bonds is the simplest one. Force fields could be used to describe and quantify H-bonding properties as, for example, the one used in the GRID software that calculates H-bonding interactions[15] by using suitable donor and acceptor probes. MolSurf is a generator of chemical descriptors from the energies of the valence electrons calculated by quantum mechanics.[16,17] However, these tools are not specifically dedicated to the computation of H-bonding properties.

The polar surface area, defined as the fraction of the molecular surface occupied by polar heteroatoms and connected hydrogen atoms, is used to describe the H-bonding properties of the molecule.[18,19] Palm and colleagues recently proposed the dynamic polar surface area (calculated as a statistical average in which the polar surface area of each low-energy conformer was weighted by its probability of existence) as a good predictor of intestinal absorption in humans. Although 3D shape and flexibility were taken into account, no distinction was made between donor and acceptor properties.[20]

To afford an improved 3D description of the H-bonding capacity, a new computational tool called the MHBPs (Molecular Hydrogen-Bonding Potentials) has been developed, consisting in a H-bonding donor potential and a H-bonding acceptor potential. The method is based on the same stepwise procedure as used previously to generate the Molecular Lipophilicity Potential (MLP).[21,22] First, a H-bonding fragmental system containing literature donor (α) and acceptor (β) values was developed, as well as geometric functions relating the variations in potential with distance and angle. The fragmental system and the geometric functions were then combined to generate the H-bonding potentials. The new computational tool has been compared with GRID interactions energies and used successfully in structure–absorption relations.[20]

MATERIAL AND METHODS

Hardware and Software

All calculations were performed on Silicon Graphics Indy R4400 175 MHz, O_2 R5000 180-MHz or Origin 2000 4•R10000 195-MHz workstations using the SYBYL 6.5 molecular modeling package (Tripos Associates, St. Louis, MO, USA) including SLN[23] (Sybyl Line Notation) and SPL (Sybyl Program Language, TSAR 3.0 (Oxford Molecular Ltd, Oxford, UK), GRID 1.5 (Molecular Discovery Ltd, Oxford, UK), SPARTAN 5.0 (Wavefunction Inc., Irvine, CA, USA) and CONCORD (CONnectivity to CoORDinates) algorithm.[24]

The Fragmental System Systahl 1.0

The fragmental system Systahl version 1.0 identifies the structural elements—polar hydrogen atoms and lone pairs—able to form H-bonds and assign a fragmental value to each of them. With this system, the total capacity of a solute to donate or accept hydrogen bonds is given by the sum of the donor or acceptor capacity of its constitutive H-bonding elements, polar hydrogen atoms or lone pairs.

Definition of H-bonds Acceptor and Donor Capacities: The fragmental system Systahl is divided into two separate parts respectively devoted to the calculation of H-bonding acceptor values β and of H-bonding donor values α for every compound.

A positive atomic H-bonding acceptor fragmental value (f_β) is associated to the pair(s) of free electrons in the polar atoms commonly encountered in medicinal chemistry and biochemistry (O,N,S, and the halogens). The association of the acceptor fragmental values to lone pairs of *polar atoms* yields a better spatial representation of the H-bonds.

Similarly, a positive atomic H-bonding donor fragmental value (f_α) is associated to each hydrogen atom connected to a polar atom (O,N, or S). They are called the *polar hydrogen atoms.*

Development of the Fragmental System Systahl: The LSER (Linear Solvation free-Energy Relationships) analysis was developed by Taft, Kamlet, Abraham, and coworkers[25–27] to factorize some given molecular properties (S_p) of neutral compounds into structural parameters such as the calculated molecular volume (V) and polar terms known as solvatochromic parameters, namely the dipolarity/polarizability π^*, the hydrogen-bonding donor acidity α, and the hydrogen-bonding acceptor basicity β. The α and β parameters can only have zero or positive values.

The scale of solute H-bonding basicity and acidity developed by Abraham and coworkers[9,10] from H-bond complexation constants in tetrachloromethane was used to build the fragmental system of H-bonding parameters called Systahl.

The solvotachromic parameters α and β determined for two series of compounds were used as starting point to build the fragmental system Systahl. The first database[9] was composed of 493 small compounds (e.g., methanol, formamide, or thiophene), while the second database[10] contained 73 medium-sized compounds (e.g., pyrazole or benzothiazole). These two databases were merged and the redundant molecules eliminated. Because no carbon atom was considered to form H-bonds even if experimentally small solvatochromic parameters were measured for nonsubstituted aromatic compounds, molecules containing no heteroatom were excluded from the database.

The geometry of all compounds was optimized using the Merck Molecular Force Field (MMFF94s).[28,29] Several steps were necessary to build and refine the fragmental system Systahl by successive iterations according to the original experimental values. The general procedure to create a molecular fragment is presented here (the same method is valid for acceptor fragments and donor fragments):

- The compounds containing only one simple chemical function (i.e., hydroxyl function) able to form H-bonds were retrieved from the database and used to built the corresponding molecular fragment. An average fragmental value was calculated for each fragment that occurs more than once.
- In case of more than one polar hydrogen atom (or polar atom), a distribution of the experimental fragmental value of the entire compound on the different polar moieties was needed. To perform this distribution, the dissociation energy of the solute–water complex was calculated using the semi-empirical Hamiltonian PM3 for several starting topologies. The total α or β fragmental value was distributed over all polar atoms or polar hydrogen atoms, respectively, in arithmetical proportion to the calculated energies.

Following this procedure, a back-calculation of the fragmental values of all compounds in the database was performed for donor and acceptor properties. A plot of experimental versus calculated values allowed to assess performance of the frag-

mental system and to identify the outliers. In a few cases, the accuracy of the fragmental system was improved by slightly modifying average fragmental values. However, due to intramolecular interactions between functional groups, the major outliers were not sufficiently well described by fragments derived from mono-functional solutes to estimate accurately their experimental H-bonding properties. Thus, Systahl was enriched with specific multifunctional fragments using also PM3 calculations to refine the distribution of the experimental value over the different polar atoms in a fragment. To maintain parametrization auto-coherence, the quality of the prediction was calculated over the entire database for every modification and/or addition.

At this stage Systahl 1.0 did not contain values for isolated polar atoms (N, O, and S) and isolated polar hydrogens connected to one polar atom (N—H, O—H, and S—H). To have such fragmental values, the fragmental values of all occurrences of these mono-atomic fragments in the database were simply averaged.

Every polyatomic fragment in Systahl 1.0 has been defined by its common name, the fragmental value associated to its polar hydrogen atoms (or its polar atoms), the SLN code describing its chemical structure, and the position of the polar hydrogens (or polar atoms) in the fragment. The SLN language allows a considerable flexibility in encoding structures. The detailed system contains 172 fragments with one or more acceptor values, 99 of which also having one or more donor values. Systahl 1.0 is available as supplementary material on the Web Site of the Institute: (http://www-ict.unil.ch/ict/systahl/systhal_index.htm).

In the Systahl 1.0 database, all fragments are ranked in decreasing order of complexity to identify first the larger and more complex fragments in a molecule. The decomposition of the analyzed compound into polyatomic fragments is achieved by SPL macro commands in the Sybyl software. The fragmental values are assigned to polar hydrogen atoms (or to polar atoms) and stored (instead of atomic partial charges) into a mol2 file type (Figure 1). For polar atoms, the fragmental value is off-centered equally on each lone pair defined as a dummy atom at a distance of 1.0 Å from the center of the polar atom. Thus, a careful definition of the atom type of each polar atom is needed. All the current Sybyl atom types satisfy the requirements except for the nitrogen atom of a pyrrole ring.

In pyrrole derivatives, the cyclic nitrogen is defined by Sybyl as a planar nitrogen without lone pairs. However the pyrrole derivatives have nonzero solvatochromic β values, prob-

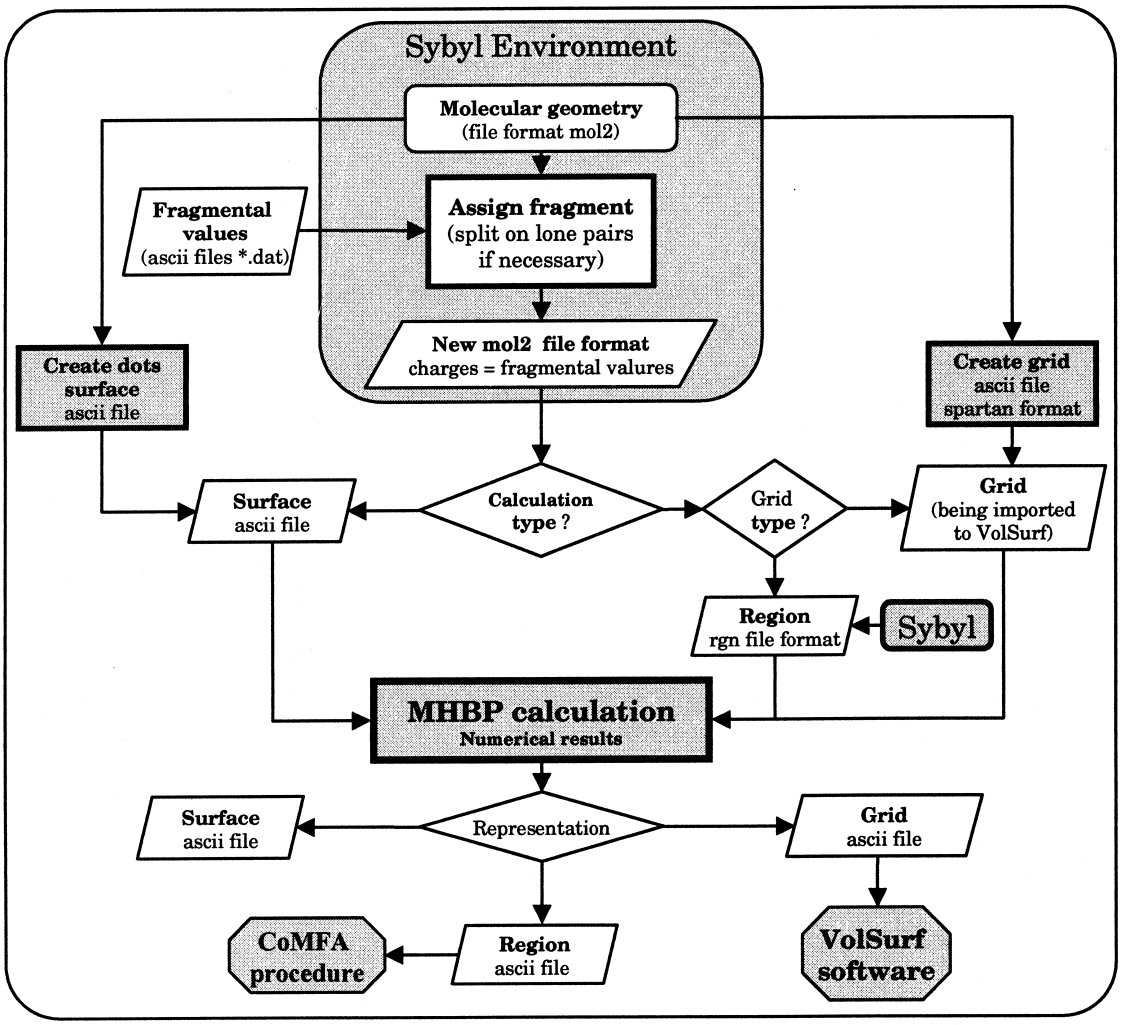

Figure 1. Algorithm of the MHBP program interfaced with the Sybyl and VolSurf software applications.

ably due to the whole cycle and not only to the nitrogen atom. As carbon atoms have no lone pairs, a solvatochromic value was attributed to the single nitrogen, defining a new atom type in Sybyl. The *N.pyr* for pyrrolic nitrogen was then added using the same characteristics as a planar nitrogen N.pl3, but with two lone pairs on both sides of the ring plane and perpendicular to it. The *N.pyr* atom type was also used in other heterocycles such as pyrazole, indazole, imidazole and pyrimidone.

Examples of Fragmental Decomposition by Systahl 1.0: The decomposition of three molecules into polyatomic fragments is presented in Figure 2 to illustrate the fragmental system Systahl 1.0. The fragments in practolol, cimetidine, and sulfafurazole are shown with their number in Systahl 1.0 and their donor and acceptor values.

The Molecular Hydrogen-Bonding Potentials (MHBPs)

Definition of the MHBPs: The MHBPs were calculated for each point k on a molecular surface (see below) or in a grid (to be computed into VolSurf) according to Eq. 1:

$$MHBP_k = \sum_{i=1}^{N_{frg}} \sum_{j=1}^{n_{at}} F_{ij} \cdot f(d_{jk}) \cdot g(U_{jk}) \qquad (1)$$

where k is the label of the point in space, N_{frg} the number of molecular fragments identified in the compound, n_{at} the number of polar atoms in the molecular fragment i, F_{ij} the α and/or β value of atom j in the fragment i, d_{jk} the distance between the polar atom j and the point k, $f(d_{jk})$ the distance function (see below), U_{jk} the angle defined by the point k, the polar atom j and the polar hydrogen or the lone pair belonging to the polar atom j, and $g(U_{jk})$ the angular function (see below). Figure 3 represents a MHBP calculation on a molecular surface. The sums of the donor and acceptor potentials on all points of the molecular surface are the two parameters for molecular H-bonding capacity (ΣMHBP) to be evaluated here in quantitative structure–permeation relationships.

Distance function: To describe how the strength of a H-bonding varies with distance, a mathematical function yielding positive values was needed.

The calculation of H-bonding interaction energies was used as starting point to find an adequate function. Commonly in molecular mechanics calculations, nonbonded interactions between two atoms are represented by a van der Waals and an electrostatic term. The Buckingham potential or the Lennard-Jones potential are commonly used to describe the potential energy associated with these terms.[30–33]

As a first approximation, the 8–6 function used in GRID[34] was inverted and tested. Nevertheless, the exponential increase of this curve for short distances is not optimal to calculate the MHBPs, because the slope in the first part of the curve is too steep and yields negative values.

Ultimately, a Gaussian function consistently yielding positive values was chosen. This function is comparable to the second part of the modified Lennard-Jones function, has a maximum at an optimal distance, and decreases sharply at shorter or higher distances. The distance function $f(d_{jk})$ for the calculation of H-bonding potentials is given by Equation 2 and illustrated in Figure 4:

$$f(d_{jk}) = e^{-\pi(d-a)^2} \qquad (2)$$

where a is the optimal distance between the polar hydrogen or polar atom and the calculated point, set to 1.8 Å as suggested by others.[35,36] A cutoff of 2.6 Å was added to the distance function to avoid unrealistic long-distance effects.

Angular function: Because H-bonds are directional, an angular function was used to describe how the potential decreases when moving away from the axis of the H-bond. A maximal value was assigned to the angle U_{jk} defined by (a) the point k in space; (b) the polar atom j (to which are attached polar hydrogen or lone pair(s)); and (c) the polar hydrogen (for a donor group) or the lone pair (for an acceptor group). The larger this angle, the smaller the MBHP potential. Some authors[37,38] have shown that this angle U_{jk} must be $<30°$ for H-bonding donor capacity and $<60°$ for H-bonding acceptor capacity. The function used to describe this behavior is given by Equation 3:

$$g(U_{jk}) = \cos\left(U_{jk} \cdot \frac{90}{max}\right) \qquad (3)$$

where U_{jk} is the angle formed by the points (a), (b), and (c) (see above), and where max is set to 30° for a donor H-bond and 60° for an acceptor H-bond. The distance function yields only positive values and points beyond these maxima are not taken into account in the MHBPs calculation.

Intramolecular Hydrogen Bonds: When polar atoms form an intramolecular H-bond, they are treated specifically and their fragmental values are modified as follows:

- When one polar atom and one polar hydrogen on different atoms are separated by a distance between 1.6 and 2.4 Å, and when the angle formed by the polar atom, the lone pair, and the polar hydrogen is in the range of 120°–180°, an intramolecular H-bond is possible and the fragmental value of the lone pair and of the polar hydrogen are set to zero (see Figure 5).
- A bifurcated intramolecular H-bond is possible between one polar hydrogen and two lone pairs, or between one lone pair and two hydrogens on another atom (e.g., lone pairs on oxygen or sulfur atoms, polar hydrogens on nitrogen atoms). Figure 6 presents the case of two polar hydrogens and one polar lone pair. To avoid topological artefacts, another geometrical condition is imposed if the previous criteria of distance and angle are satisfied, namely an angle $<55°$ between the center M of the segment formed by the two lone pairs or the two hydrogens, the polar atom bearing them, and the polar hydrogen or lone pair (see Figure 6). The fragmental value of the polar hydrogen or lone pair is then set to zero, while the fragmental values of the two lone pairs or polar hydrogens are divided by two.

This procedure allows major intramolecular H-bonds to be taken into account when computing MHBPs.[32,39]

Molecular surface of computation: To represent the MHBPs corresponding to the maximal H-bonding potential, a Surface of H-Bonding (SHB) was defined. This SHB was located 1.8 Å from the center of each atom in the molecule.

Algorithm to compute the MHBPs: A program was written in C to determine intramolecular H-bonds and to calculate the MHBPs. Two data files are needed to this end, one gener-

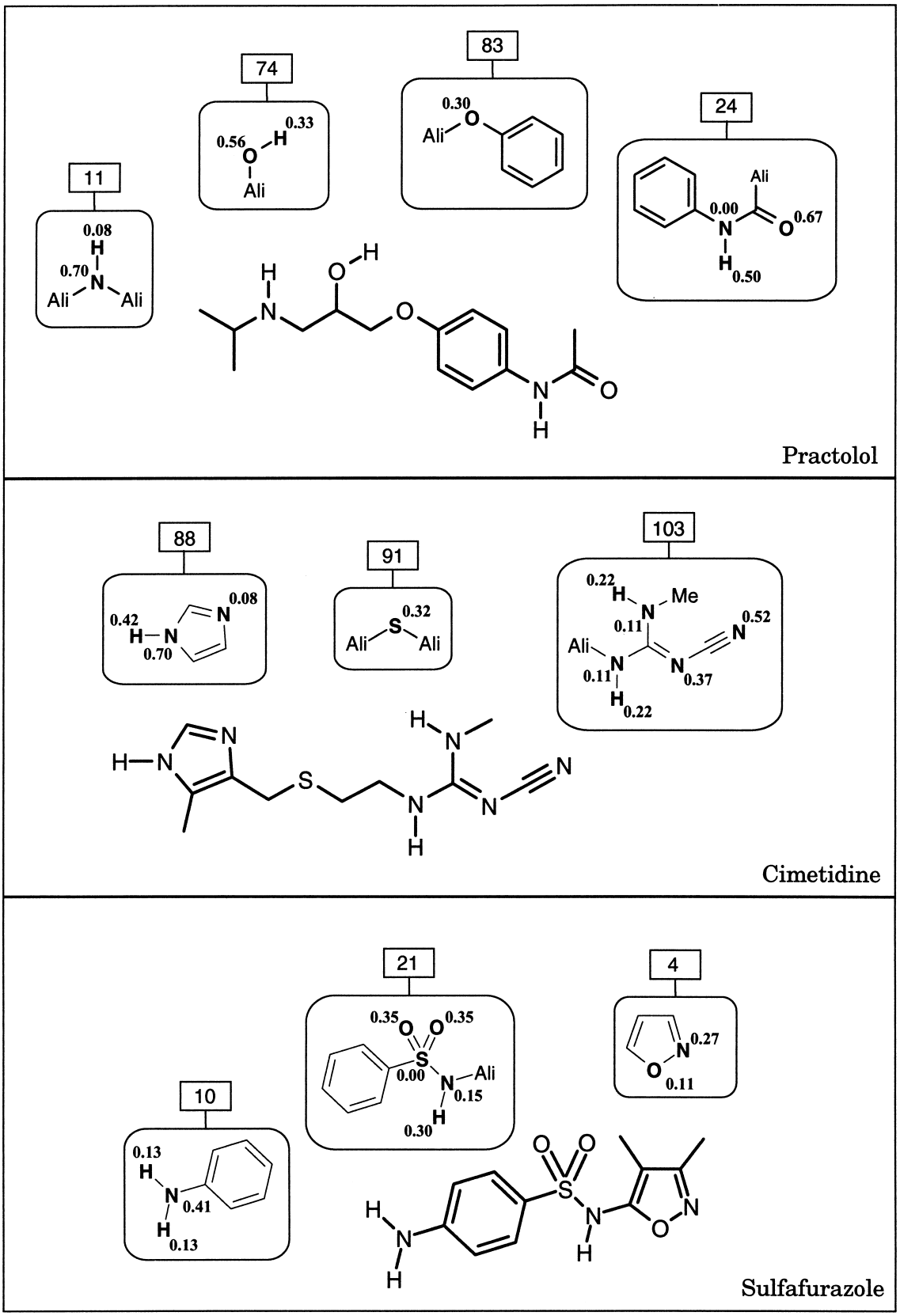

Figure 2. Representation of the Systahl 1.0 fragmental decomposition of practolol, cimetidine, and sulfafurazole. For each polyatomic fragment the fragmental value for the considered polar atoms and the number of the fragment are shown. The donor (or acceptor) fragmental sum is 0.91 (acceptor, 2.23) for practolol, 0.86 (2.21) for cimetidine, and 0.56 (1.64) for sulfafurazole.

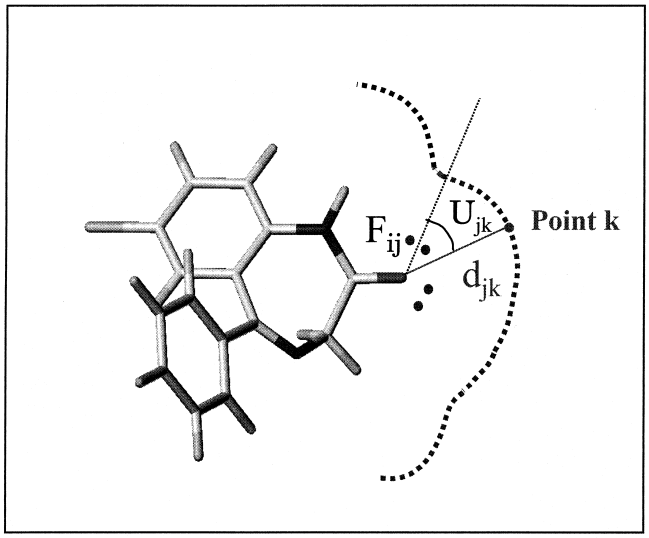

Figure 3. Representation of the MHBPs calculation on a molecular surface.

ated by Sybyl and containing the molecular geometry plus the fragmental values, and another containing the coordinates of the points where the MHBPs will be calculated. To enhance the versatility of the software, the set of these points was defined so that it could belong to either of three different objects:

- a molecular surface (the SHB) generated from the molecular geometry by a program written in C;
- a 3D grid, as defined in CoMFA, to allow inclusion of an additional field in 3D-QSAR analyses;
- a 3D grid in the SPARTAN format, generated from the molecular geometry by a program written in C, to allow analysis by external tools such as VolSurf[40] or GOLPE.[41]

The Sybyl software was used via a small retrieval interface to represent the MHBPs only for the points with nonzero ΣMHBP values. This feature allows a visual comparison of the H-bonding capacity of different compounds. The algorithm of the MHBPs software is shown in Figure 1.

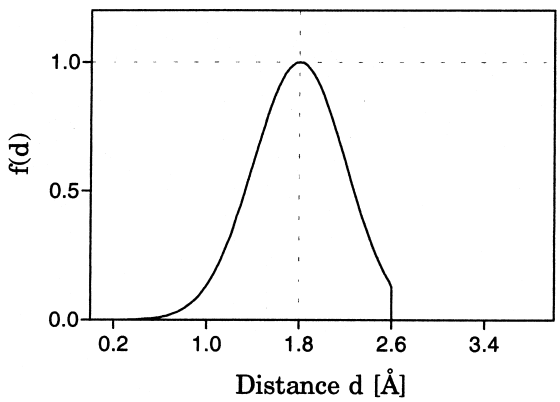

Figure 4. Graph of the distance function, with cutoff at 2.6 Å and unitary value at a distance of 1.8 Å.

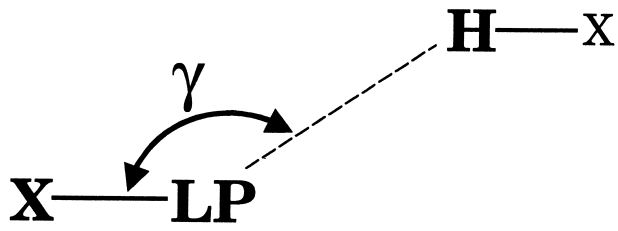

Figure 5. Representation of the angle (γ) formed by the polar atom, the lone pair, and the polar hydrogen in case of intramolecular H-bond.

Log P Data

The log P and log $D^{7.4}$ (i.e., the octanol/water partition coefficient of neutral species, and the distribution coefficient at pH 7.4) are of relevance in this study and were obtained from the MedChem database[42] or calculated by the CLOGP algorithm.[42]

The log P value of diazepam (**4**), mannitol (**7**), nordazepam (**10**), oxazepam (**12**), and phenazone (**14**) (which is identical to their log D value) was obtained from the MedChem database. An experimental log D value reported in the literature was used for ciprofloxacin (**3**), sulpiride (**19**), and foscarnet (**5**).[20] The log P value of lactulose (**6**), raffinose (**17**), and practolol (**16**) was calculated by the CLOGP algorithm,[42] and for the latter compound it was corrected for ionization at pH = 7.4 (CLOGD). No reliable octanol/water distribution coefficient could be obtained for metolazone (**8**), olsalazine (**11**), sulfasalazine (**18**), and tranexemic acid (**20**), and these four drugs were removed from the study. The lipophilicity data of the β-blockers (alprenolol (**1**), atenolol (**2**), metoprolol (**9**), oxprenolol (**13**), and pindolol (**15**) were published values.[43]

Quenched Molecular Dynamics (QMD)

A simplified conformational search strategy[44,45] was adopted that is able to describe efficiently the main valleys of a conformational space. The starting geometries were built by CONCORD and energy-optimized using the MMFF94s Field in-

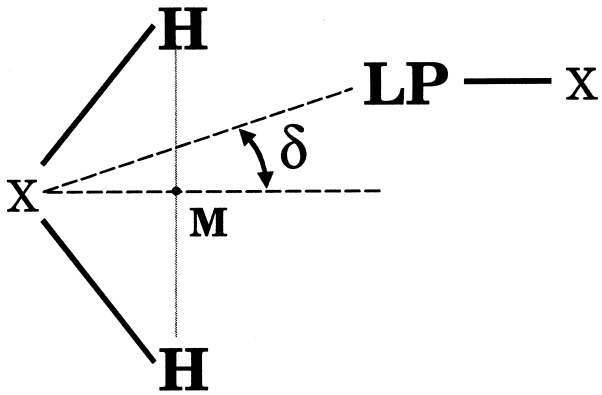

Figure 6. Representation of the angle (δ) formed by the polar lone pair attached to a polar atom, the other polar atom bearing two polar hydrogens atom, and the center M of the segment formed by the two polar hydrogens atoms.

cluding MMFF94 partial atomic charges to remove initial high-energy interactions.

High-temperature molecular dynamics (MD) calculations were carried out at 2000 K. Each simulation was run for 100 ps with steps of 1.0 fs. The frame data were stored every 0.05 ps, giving 2,000 frames. The starting velocities were calculated from a Boltzmann distribution. Finally, 10% of all conformers were randomly selected and saved in a database ultimately containing about 200 conformers.

All conformers in the database were then subjected to energy minimization using the same force field as for the MD calculations,[46] and the conformational similarity of the energy-minimized conformers was investigated by comparing all pairs of conformers.[46]

Calculation of the Polar Surface Area (SACPOL)

Water-accessible surface areas (SASA) were calculated with the program MOLSV (QCPE No. 509). Van der Waals radii were taken from Gavezzotti,[47] and the H_2O molecule was assumed to be a sphere of 1.5 Å radius. The H_2O-accessible surface area was calculated as the ensemble of all points encountered by the center of the water sphere when rolling on the molecular surface. The polar surface area (SACPOL) was defined as the fraction of the SASA occupied by polar atoms (nitrogen, oxygen, sulfur, and phosphorus) and hydrogen atoms attached to them. For a given molecule $SACPOL^{Min}$ and $SACPOL^{Max}$ are respectively the smallest and the largest values of the polar surface area found by calculating the SACPOL on the final database of conformers obtained by QMD (see above). $SACPOL^{Con}$ is the polar surface area calculated for each compound on an averaged 3D structure generated by CONCORD and minimized by the MMFF94s force field.

Molecular Descriptors Generated by the GRID Program[15]

In the GRID program,[34,48,49] the sum of steric, electrostatic, and H-bonding energies between a compound and a probe yields a negative field for attractive interactions and a positive field for repulsive interactions at each point of a lattice of variable size.[38] Different probes corresponding to different types of interactions can be used. Here, the H-bonding donor and acceptor properties of the solutes were calculated using the following probes:

- The probes for H-bonding were a carbonyl group able to accept two hydrogen bonds (the acceptor probe), and an amide group able to donate two hydrogen bonds (the donor probe).
- To exclude steric and electrostatic effects, the probes were defined as a single point in space with zero charge. As a result, the calculated energy represents the H-bonding energy (E_{Hb}) only, expressed in kcal mol^{-1}.

The GRID software offers additional possibility, namely to take into account rotational flexibility around single bonds. Thus to extend the possibilities of comparison between GRID and the MHBPs, the fixed and flexible GRID interactions energies were calculated. The different graphical representations available in Sybyl were used for a visual, qualitative comparison between GRID energies and the MHBPs.

VALIDATION OF THE MHPBS

Validation of the Fragmental System Systahl 1.0

The good performance of the fragmental system Systahl version 1.0 was confirmed by linear correlations between the experimental solvatochromic values (donor and acceptor capacity) and the sum of the fragmental values obtained with Systahl on the compounds used to built the fragmental system (Figure 7A and 7B). In both correlations, some compounds characterized by the lack of polar atom (e.g., benzene and alkanes structure) were omitted.

Visual Comparison between MHBPs and GRID Interaction Energies

The MHBPs and GRID interaction energies can be calculated at each point in 3D space. These fields were compared visually to select the best method to transform them into 3D-descriptors usable in QSAR studies. When GRID interactions energies were restricted to their H-bonding component (see Materials and Methods), a comparison with the MHBPs became possible. Color plates 1, 2, and 3 illustrate the H-bonding donor and acceptor properties of nordazepam (**10**), atenolol (**2**), and mannitol (**7**), respectively, as calculated by the MHBPs and GRID. Flexible GRID interactions (by default in the software) were determined for the three molecules, and fixed GRID interactions only for mannitol (**7**). In both cases, a three-colors scale (red, orange, and yellow) was used to represent iso-potential contours, red coding for the maximal H-bonding capacity, and yellow for the minimal capacity. In these figures, the SHB molecular surface is represented in green while the water accessible-surface area is in magenta.

Nordazepam (**10**) (Color Plate 1) is a rigid compound possessing one H-bonding donor and two H-bonding acceptor groups. Whereas the two methods gave comparable results, two differences can nevertheless be seen:

- Due to the restricted angular conditions, the MHPBs regions are more localized than GRID regions.
- Due to a different distance functions, the MHBPs regions are closer to the polar elements. In particular, the H-bonding acceptor regions are more localized around lone pairs.

For atenolol (**2**) (Color Plate 2), the molecular fields display the same differences. In addition, in the chosen conformer, the hydroxyl group in the side-chain forms an intramolecular H-bonding with the ether oxygen atom. The specific treatment of intramolecular H-bonds in the MHBPs assigns zero H-bonding donor capacity to this OH group and a lowered H-bonding acceptor capacity to the ether function, in contrast to GRID which calculates discrete energies even for internal H-bonds.

A similar behavior can be noted for mannitol (**7**) (Color Plate 3), a flexible compound forming several intramolecular H-bonds. Interestingly, GRID energies here are sensitive to the different topologies of internal H-bonds, yielding different H-bonding capacities to the various polar hydrogens and to the oxygen atoms. When the rotational flexibility of the hydroxyl function (see Material and Methods) was used in the calculation of GRID energies (Color Plate 3, lower panel), the H-bonding regions appeared largely delocalized in the 3D space.

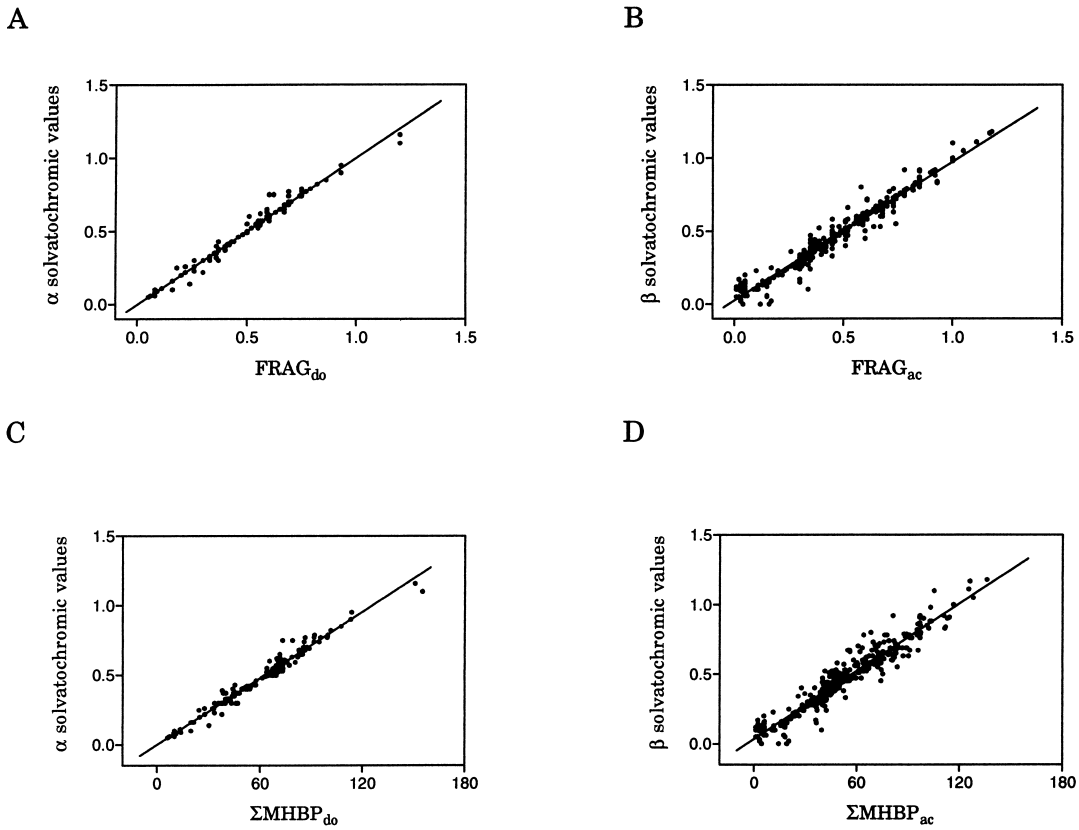

Figure 7. Correlation between the experimental solvatochromic values and the fragmental values calculated by Systahl 1.0: A indicates the donor capacity of H-bonding ($FRAG_{do}$, $r^2 = 0.98$); B, the acceptor capacity of H-bonding ($FRAG_{ac}$, $r^2 = 0.96$). Correlation between the experimental solvatochromic values and the MHBPs: C indicates the donor capacity of H-bonding ($\Sigma MHBP_{do}$, $r^2 = 0.98$); D, the acceptor capacity of H-bonding ($\Sigma MHBP_{ac}$, $r^2 = 0.93$).

As a consequence of the distance function used in the MHBPs, the Surface of H-Bonding (SHB) cuts through the region of maximal H-bonding capacity, whereas the water-accessible surface area is too distant to encode a discrete H-bonding capacity. The dot representation of the MHBPs on the SHB reproduces well the features of iso-potential contours (Color Plate 4).In analogy with the MLP methodology,[21,22] it thus appears that integrating the MHPBs on the SHB yields a fair, conformation-dependent 3D global representation of the total H-bonding capacity of a solute.

For the GRID energies, the two molecular surfaces (SHB molecular surface and water accessible-surface area) do not correspond to the maximum of the H-bonding interactions. Thus, integrating on these surfaces would yield biased values containing only a portion of the total interaction energies. Other techniques such as VolSurf[40] appear better suited to extract 3D molecular parameters from the energies calculated by the GRID program.

Integration of the MHBPs on the SHB

The integration of the MHBPs in a finite space (the SHB) should quantify the total capacity of a solute to donate and accept H-bonds. This integration was achieved by summing the potential on all points of the SHB, obtaining two molecular parameters called $\Sigma MHBP_{do}$ and $\Sigma MHBP_{ac}$ which are taken to represent the total H-bonding donor and acceptor capacity, respectively. The $\Sigma MHBP_{do}$ and $\Sigma MHBP_{ac}$ depend on the 3D structure (and hence the conformation) of the compounds, and as demonstrated in Figure 7C and 7D they are highly correlated with the α and β solvatochromic parameters used as starting values. In other words, the $\Sigma MHBP_{do}$ and $\Sigma MHBP_{ac}$ allow the back-calculation of the total α and β values of a solute, and hence its H-bonding donor and acceptor capacity, like the MLP allows the back-calculation of log P.

A difference is that the MHBPs are more localized than the MLP. Also, the back-calculation of the total H-bonding capacity from the MHBPs is of little interest for small solutes with limited flexibility.

APPLICATION OF THE MHBPS TO STRUCTURE-ABSORPTION RELATIONS

Having developed a method to calculate the H-bonding donor and acceptor capacity from 3D structure, it was important to examine the applicability of the derived parameters in quantitative structure–activity relationships, more specifically in quantitative structure–absorption relationships. To this end, we have used the dataset reported by Palm and colleagues,[20] which contains the oral absorption in humans of a set of therapeutic and model compounds (see Table 1).

Table 1. Human fraction absorption and structural properties of investigated drugs

	Compounds	ABS [%][a)]	log $D^{7.4}$ [b)]	$SACPOL^{Con}$ [c)]	$SACPOL^{Max}$ [c)]	$SACPOL^{Min}$ [c)]
1	Alprenolol	96.0	0.99	51.8	74.7	35.5
2	Atenolol	54.0	−1.92	172.8	185.1	167.2
3	Ciprofloxacin	69.0	−1.11	212.1	213.5	190.8
4	Diazepam	97.0	2.99	75.7	75.3	75.3
5	Foscarnet	17.0	−1.78	260.2	260.4	255.5
6	Lactulose	0.6	−5.69	334.2	374.0	299.1
7	Mannitol	26.0	−3.10	247.4	254.6	205.7
8	Metolazone	64.0	–	183.2	183.4	180.9
9	Metoprolol	102.0	−0.22	104.0	125.0	88.1
10	Nordazepam	99.0	2.93	96.1	72.5	72.5
11	Olsalazine	2.3	–	313.4	335.6	311.1
12	Oxazepam	97.0	2.24	132.4	132.3	132.3
13	Oxprenolol	97.0	0.46	70.4	81.7	48.0
14	Phenazone	97.0	0.38	64.2	64.0	64.0
15	Pindolol	92.0	−0.27	126.0	145.0	120.7
16	Practolol	95.0	−0.97	130.5	149.8	115.9
17	Raffinose	0.3	−8.09	437.4	457.5	364.5
18	Sulfasalazine	12.0	–	293.3	313.1	275.6
19	Sulpiride	36.0	−1.15	206.9	226.5	206.6
20	Tranexemic acid	55.0	–	161.8	163.1	136.2

[a] Oral drug absorption (in %) taken from Palm et al.[20]
[b] See text for the origin of these lipophilicity data.
[c] Polar Surface Area defined as the fraction of the SASA occupied by polar atoms (nitrogen, oxygen, sulfur and phosphorus) and hydrogen atoms attached to them. $SACPOL^{Con}$ values were obtained on an averaged 3D structure generated by CONCORD.[24] $SACPOL^{Max}$ and $SACPOL^{Min}$ are the maximal and minimal SACPOL values, respectively, found among all conformers obtained by QMD.

Global Parameters

pH-dependent lipophilicity descriptors: Various studies have revealed a variety of relations (linear, parabolic, sigmoidal) between absorption and log P, depending on the dataset examined. In contrast, highly heterogeneous series of compounds yielded poorer correlations.[20] For example, no relation was found between absorption and CLOGP in a series of drugs of which some were partly or completely ionized at physiological pH,[20] perhaps due to the fact that lipophilicity data were used without correction for ionization (i.e., log P of the neutral species). The lipophilicity data were carefully analyzed and their relationships with absorption data reexamined here.

A sigmoidal relationship between log $D_{oct}^{7.4}$ and absorption (Figure 8A, $r^2 = 0.87$) was obtained when the distribution coefficients at physiological pH (log $D_{oct}^{7.4}$, see above) were used revealing that the percentage of ionized forms present at physiological pH is an important factor linked to membrane permeation.

Polar surface areas and the role of conformation in the calculation of theoretical parameters: Palm and colleagues[20] recently proposed the polar surface area as a good predictor of intestinal absorption in humans. This molecular parameter was calculated as a statistical average in which the surface area of each low-energy conformer was weighted by its probability of occurrence. But because the biological environment in the body is very different from the gas phase conditions used in the calculations, it may be misleading to consider only low-energy gas-phase conformers.[50–52]

To check the influence of flexibility on the calculation of theoretical parameters, a QMD study of the complete conformational space of the compounds in their neutral form was performed, and the corresponding surface parameters were calculated (see Materials and Methods) and correlated with absorption data.

The relationships between (a) the polar surface area calculated on an averaged 3D structure ($SACPOL^{Con}$), and (b) the smallest or largest value of the polar surface area ($SACPOL^{Min}$ and $SACPOL^{Max}$) (Table 1) are shown in Figures 8B and 8C. The good linear relations ($r^2 = 0.97$ and $r^2 = 0.97$, respectively) indicate that at least in this series, the relevance of conformational flexibility is negligible.

The sigmoidal relation between absorption and $SACPOL^{Con}$ (Figure 8D) confirms that the polar surface area is indeed of value as a predictor of membrane permeability. However, the SACPOL parameters encode a variety of intermolecular forces, as confirmed by the linear relation between $SACPOL^{Con}$ and log $D^{7.4}$ ($r^2 = 0.83$, graph not shown).[53] Thus, these parameters will fail to afford mechanistic insights into the recognition forces controlling membrane permeation.

Molecular hydrogen-bonding potentials: To explore how the H-bonding capacity varies in the conformational space of each compound, the donor and acceptor MHBPs ($\Sigma MHBP_{do}$ and $\Sigma MHBP_{ac}$, respectively) were calculated for all conformers obtained by QMD. The maximal ($\Sigma MHBP^{Max}$), minimal ($\Sigma MHBP^{Min}$) and weighted average ($\Sigma MHBP^{Wav}$) values are listed in Table 2 and Table 3. The weighted average was calculated according to Equation 4.

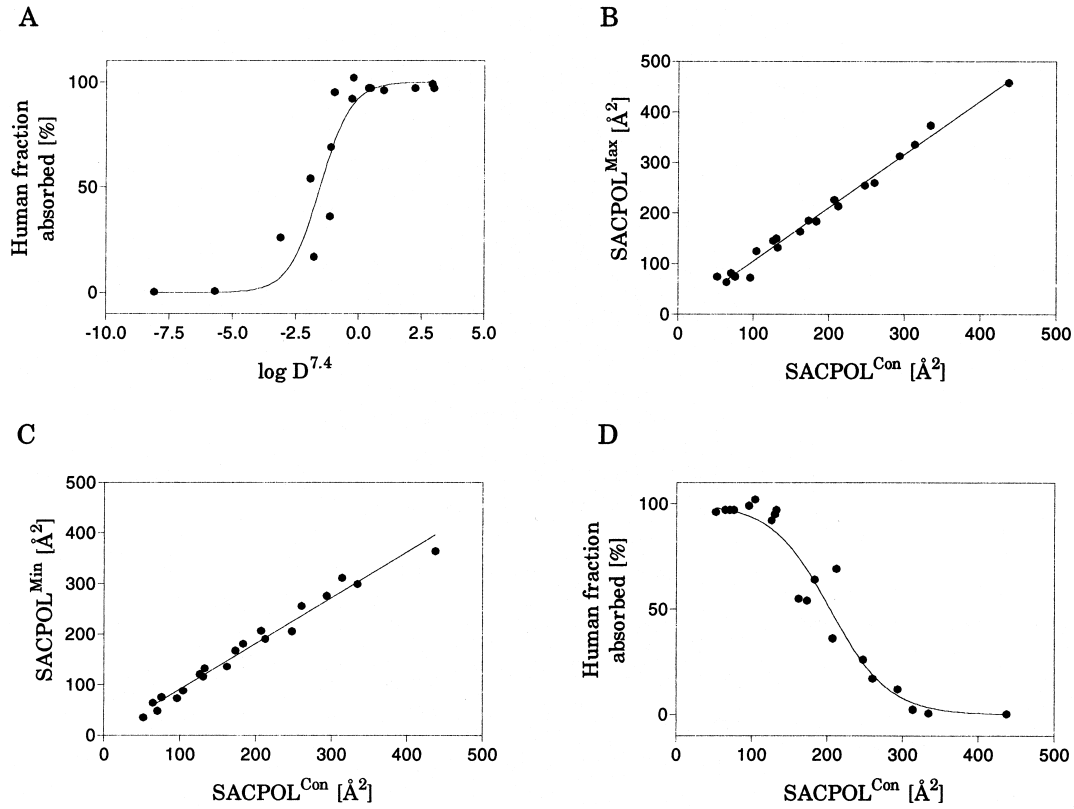

Figure 8. Lipophilicity–absorption relationships: A indicates sigmoidal relationship between the fraction of dose absorbed orally in humans and the distribution coefficient in octanol/water at physiological pH (log $D^{7.4}$). B, linear relationship between $SACPOL^{Max}$ (the maximal polar surface area found among all conformers obtained by QMD) and $SACPOL^{Con}$ (the polar surface area calculated on an averaged 3D-structure generated by CONCORD). C, linear relationship between $SACPOL^{Min}$ (the minimal polar surface area value found among all conformers obtained by QMD) and $SACPOL^{Con}$ (the polar surface area calculated on an averaged 3D-structure generated by CONCORD). D, Sigmoidal relationship between the fraction of dose absorbed orally in humans and $SACPOL^{Con}$ (the polar surface area calculated on an averaged 3D-structure generated by CONCORD).

$$WA = \frac{\sum_{i=1}^{N_{conf}} (x_1)^2}{\sum_{i=1}^{N_{conf}} x_i} \qquad (4)$$

where N_{conf} is the number of conformers and x_i the donor or acceptor MHBPs value calculated for the conformer i. In addition, the calculation of the $\Sigma MHBP^{Con}$ was performed for the starting geometries built by CONCORD and minimized with the MMFF94s force field.

In this small set of compounds, the minimal and the maximal ΣMHBP differ more in H-bonding donation (Figure 9A) than in H-bonding acceptance (Figure 9B). In fact, the minimal values of the ΣMHBP correspond to the conformers with the largest number of intramolecular H-bonds, and the maximal values to conformers with the smallest number of intramolecular H-bonds. The variation of the MHBPs in the conformational space is mostly due to the change in fragmental values resulting in intramolecular H-bonds rather than in large variations of the SHB. The effect of intramolecular H-bonds is felt more by the $\Sigma MHBP_{do}$ than the $\Sigma MHBP_{ac}$ since, in this limited series, the number of polar hydrogens is much smaller than the number of heteroatoms.

The maximal values of the parameters are highly correlated with the weighted average $\Sigma MHBP^{Wav}$ for H-bonding acceptor capacity (Figure 9D), and partially correlated with H-bonding donor capacity (Figure 9C). The $\Sigma MHBP^{Min}$ in both cases have low statistical weight except for compounds with several intramolecular H-bonds, namely lactulose (**6**), mannitol (**7**), olsalazine (**11**), and raffinose (**17**).

The relationship between the $\Sigma MHBP^{Wav}$ and the $\Sigma MHBP^{Con}$ for donor capacity (Figure 9E) and acceptor capacity (Figure 9F) indicate that 3D average structures given by the CONCORD algorithm can be used to approximate ΣMHBP.

Here, the different ΣMHBP parameters were examined for their relation with data of oral absorption in humans. The following results were obtained:

- For the H-bonding acceptor capacity, no relationship was found as illustrated by the plot of human absorption versus $\Sigma MHBP_{ac}{}^{Con}$ (Figure 10B).
- For the H-bonding donor capacity, sigmoidal relationships of similar statistical quality link the fraction absorbed to $\Sigma MHBP_{do}{}^{Max}$, $\Sigma MHBP_{do}{}^{Con}$ or $\Sigma MHBP_{do}{}^{Wav}$, while no relationship is apparent with $\Sigma MHBP_{do}{}^{Min}$ (graphs not shown). Figure 10A summarizes these results

Table 2. Donor molecular hydrogen-bonding potentials of investigated drugs[a)]

	Compounds	$\Sigma MHBP_{do}^{Min\ b)}$	$\Sigma MHBP_{do}^{Max\ c)}$	$\Sigma MHBP_{do}^{Wav.\ d)}$	$\Sigma MHBP_{do}^{Con\ e)}$
1	Alprenolol	0.0	52.1	39.5	10.7
2	Atenolol	74.2	129.7	111.4	86.0
3	Ciprofloxacin	0.0	85.5	81.8	83.3
4	Diazepam	0.0	0.0	0.0	0.0
5	Foscarnet	121.9	191.0	166.6	188.4
6	Lactulose	84.3	264.9	199.5	183.0
7	Mannitol	46.6	206.4	150.3	127.3
8	Metolazone	99.6	104.2	101.9	102.0
9	Metoprolol	0.0	56.5	43.1	10.7
10	Nordazepam	66.6	66.6	66.6	67.3
11	Olsalazine	138.5	285.8	212.4	145.7
12	Oxazepam	106.7	106.7	106.7	108.1
13	Oxprenolol	0.0	55.4	41.5	10.5
14	Phenazone	0.0	0.0	0.0	0.0
15	Pindolol	34.2	88.5	76.1	44.8
16	Practolol	74.6	122.4	104.2	79.0
17	Raffinose	82.7	341.0	212.4	176.7
18	Sulfasalazine	109.1	182.4	143.1	115.9
19	Sulpiride	67.1	117.1	91.6	111.4
20	Tranexemic acid	93.0	99.1	96.3	96.5

[a] Donor H-bonding properties as calculated by the Molecular Hydrogen-Bonding Potentials (MHBPs). The smaller the values of ΣMHBP potentials, the weaker the HB power.
[b,c] Mimimal (resp. maximal) value of ΣMHBP found among all conformers obtained by QMD.
[d] Weighted average value of ΣMHBP calculated for all conformers according to Eq. 4.
[eΣ] MHBP value calculated on an averaged 3D structure generated by CONCORD.[24]

Table 3. Acceptor molecular hydrogen-bonding potentials of investigated drugs[a)]

	Compounds	$\Sigma MHBP_{ac}^{Min\ b)}$	$\Sigma MHBP_{ac}^{Max\ c)}$	$\Sigma MHBP_{ac}^{Wav.\ d)}$	$\Sigma MHBP_{ac}^{Con\ e)}$
1	Alprenolol	78.3	167.05	187.89	155.9
2	Atenolol	172.5	260.7	286.4	241.3
3	Ciprofloxacin	156.7	190.6	204.5	184.3
4	Diazepam	105.0	105.0	122.6	105.1
5	Foscarnet	131.6	157.8	161.8	157.6
6	Lactulose	447.5	596.5	639.8	490.2
7	Mannitol	210.2	297.6	324.5	239.9
8	Metolazone	151.9	167.3	184.0	155.8
9	Metoprolol	134.5	241.7	257.0	214.3
10	Nordazepam	115.2	115.2	128.6	114.3
11	Olsalazine	133.5	152.0	154.1	142.9
12	Oxazepam	181.0	181.0	200.1	177.5
13	Oxprenolol	107.6	212.0	226.9	192.5
14	Phenazone	64.1	64.8	76.6	64.8
15	Pindolol	93.1	187.9	197.8	160.4
16	Practolol	155.9	259.4	270.3	218.7
17	Raffinose	566.1	750.8	886.8	709.5
18	Sulfasalazine	209.1	227.1	239.3	216.0
19	Sulpiride	189.5	283.8	308.5	273.7
20	Tranexemic acid	110.9	122.4	134.2	115.8

[a] Acceptor H-bonding properties as calculated by the Molecular Hydrogen-Bonding Potentials (MHBPs). The smaller the values of ΣMHBP potentials, the weaker the HB power.
[b,c] Minimal (resp. maximal) value of ΣMHBP found among all conformers obtained by QMD.
[d] Weighted average value of ΣMHBP calculated for all conformers according to Eq. 4.
[e] ΣMHBP value calculated on an averaged 3D structure generated by CONCORD.[24]

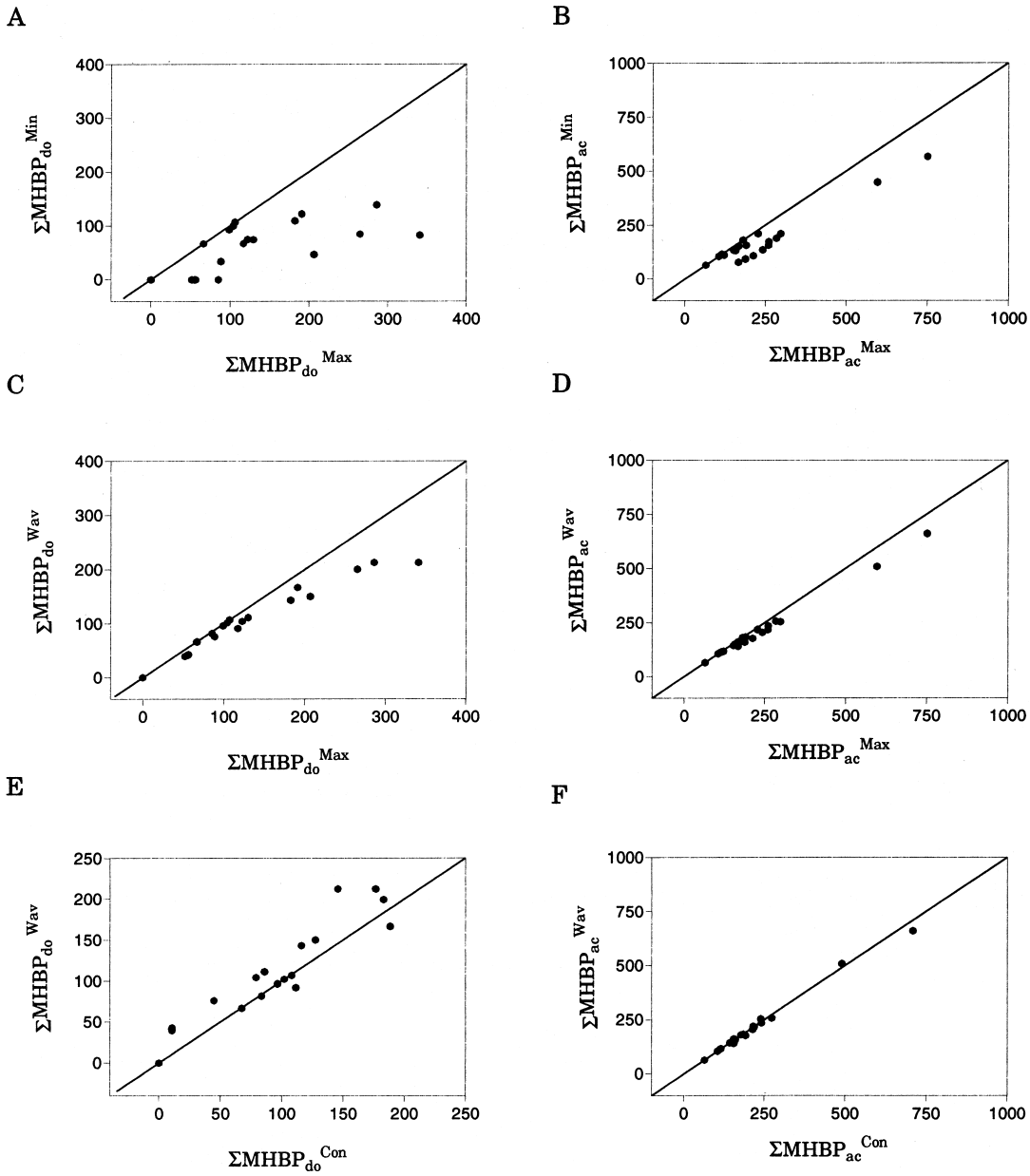

Figure 9. H-bonding–absorption relationships: A indicates linear relationship between the minimal H-bonding donor potentials ($\Sigma MHBP_{do}^{Min}$) and the maximal H-bonding donor potentials ($\Sigma MHBP_{do}^{Max}$); B, linear relationship between the minimal H-bonding acceptor potentials ($\Sigma MHBP_{ac}^{Min}$) and the maximal H-bonding acceptor potentials ($\Sigma MHBP_{ac}^{Max}$). C, linear relationship between the weighted H-bonding donor potentials ($\Sigma MHBP_{do}^{Wav}$) and the maximal average H-bonding acceptor potentials ($\Sigma MHBP_{do}^{Max}$). D, linear relationship between the weighted H-bonding acceptor potentials ($\Sigma MHBP_{ac}^{Wav}$) and the maximal average H-bonding acceptor potentials ($MHBP_{ac}^{Max}$). E, linear relationship between the weighted H-bonding donor potentials ($\Sigma MHBP_{do}^{Wav}$) and the Concord average H-bonding acceptor potentials ($\Sigma MHBP_{do}^{Con}$). F, linear relationship between the weighted H-bonding acceptor potentials ($\Sigma MHBP_{ac}^{Wav}$) and the Concord average H-bonding acceptor potentials ($\Sigma MHBP_{ac}^{Con}$).

by representing the sigmoid generated for $\Sigma MHBP_{do}^{Con}$ and the variation in H-bonding donor capacity over the conformational space symbolized by the horizontal segments joining the minimal and maximal ΣMHBP values.

This study underlines several interesting features:

- The H-bonding donor capacity, but not the H-bonding acceptor capacity, appears to be able to predict oral absorption. This is in agreement with the major influence of the H-bonding donor acidity on drug absorption as revealed by the ratio of H-bond donor and H-bond acceptor groups in the Pfizer's rules.[54]
- In the set of compounds examined here, conformational effects are mainly associated by the presence or absence of intramolecular H-bonds. The conformers with all possible

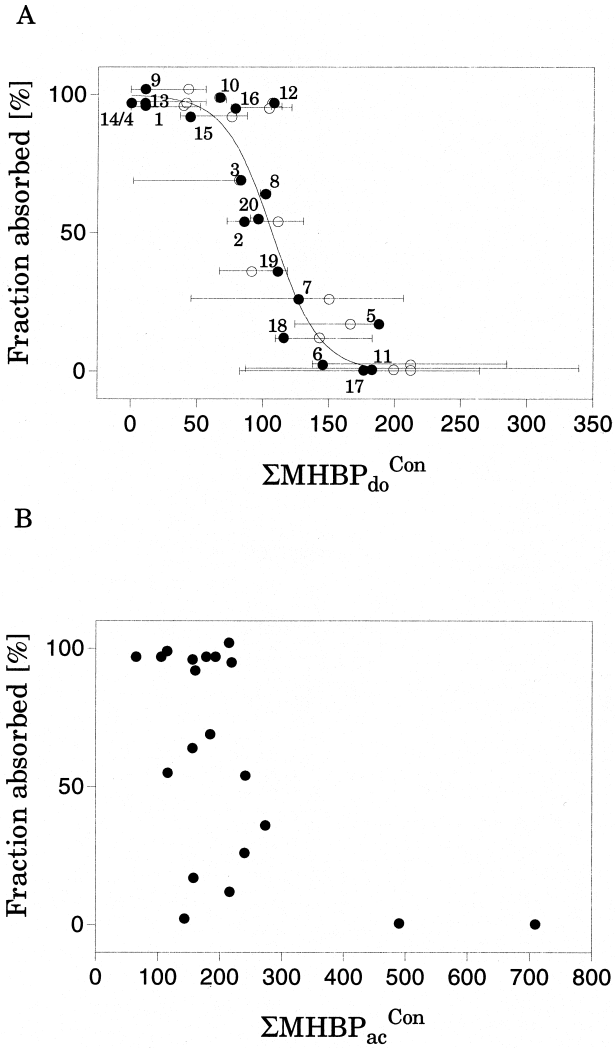

Figure 10. Relationship between the fraction of dose absorbed orally in humans and: A, the CONCORD H-bonding donor potentials ($\Sigma MHBP_{do}^{Con}$); B, the CONCORD H-bonding acceptor potentials ($\Sigma MHBP_{ac}^{Con}$).

intramolecular H-bonds are inappropriate to predict oral absorption, in contrast to the conformers with the minimum number of intramolecular H-bonds. However, there was no correlation between the ranking of conformers according to their gas-phase energy and to their H-bonding donor capacity. The best correlations with oral absorption are obtained with $\Sigma MHBP_{do}^{Max}$ or $\Sigma MHBP_{do}^{Wav}$, i.e., the H-bonding donor capacity of the conformers without internal H-bonds.

- Interestingly, the predictions with parameters obtained from 3D structures generated by the CONCORD algorithm are similar to the predictions given by $\Sigma MHBP_{do}^{Max}$ or $\Sigma MHBP_{do}^{Wav}$. Thus, the computationally heavy step of conformational analysis does not appear necessary in estimating oral absorption. This validates the use of the fast CONCORD algorithm in the virtual screening of large series of candidates.

CONCLUSIONS

The MHBPs presented here are empirical tools able to compute and display the 3D hydrogen bonding potentials of compounds as a function of their conformation and topography. The influence of intramolecular H-bonds on conformational behavior is well evidenced by the range of ΣMHBP values, and particularly $\Sigma MHBP_{do}$. Interestingly, average 3D structures generated by CONCORD are suitable for fast prediction of oral human absorption.

The promising results obtained with the MHBPs are considered as a starting point for further analysis. It must also be noted that because of the strongly directional character of the H-bond, the choice of the best molecular surface on which to compute H-bonding properties is crucial. The benefits of using MHBPs in a GRID or as an additional field in CoMFA are currently being explored.

ACKNOWLEDGMENTS

BT and PAC acknowledge support by the Swiss National Science Foundation.

REFERENCES

1 Williams, D.H. The molecular basis of biological order. *Aldrichim. Acta* 1991, **24**, 71–80
2 Tsai, R.S., El Tayar, N., Carrupt, P.A., and Testa, B. Physicochemical properties and transport behavior of piribedil: considerations on its membrane-crossing potential. *Int. J. Pharm.* 1992, **80**, 39–49
3 Abraham, M.H., Chadha, H.S., and Mitchell, R.C. The factors that influence skin penetration of solutes. *J. Pharm. Pharmacol.* 1995, **47**, 8–16
4 Houk, J., and Guy, R.H. Membrane models for skin penetration studies. *Chem. Rev.* 1988, **88**, 455–471
5 Pugh, W.J., and Hadgraft, J. Ab initio prediction of human skin permeability coefficients. *Int. J. Pharm.* 1994, **103**, 163–178
6 El Tayar, N., Tsai, R.S., Testa, B., Carrupt, P.A., Hansch, C., and Leo, A. Percutaneous penetration of drugs: a quantitative structure– permeability relationship study. *J. Pharm. Sci.* 1991, **80**, 744–749
7 Chikhale, E.G., Ng, K.Y., Burton, P.S., and Borchardt, R.T. Hydrogen bonding potential as a determinant of the in vitro and in situ blood–brain barrier permeability of peptides. *Pharm. Res.* 1994, **11**, 412–419
8 Testa, B., El Tayar, N., Altomare, C., Carrupt, P.A., Tsai, R.S., and Carotti, A. The hydrogen bonding of drugs: its experimental determination and role in pharmacokinetics and pharmacodynamics. In: *Trends in Receptor Research.*, Angeli, P., Gulini, U., and Quaglia, W., Eds., Elsevier, Amsterdam, 1992, 18, pp. 61–72
9 Abraham, M.H. Hydrogen bonding. 31. Construction of a scale of solute effective or summation hydrogen-bond basicity. *J. Phys. Org. Chem.* 1993, **6**, 660–684
10 Abraham, M.H., Chadha, H.S., and Mitchell, R.C. Hydrogen bonding. 33. Factors that influence the distribution of solutes between blood and brain. *J. Pharm. Sci.* 1994, **83**, 1257–1268
11 Raevsky, O.A. Hydrogen bond strength estimation by means of the HYBOT program package. In: *Computer-Assisted Lead Finding and Optimization. Current Tools for Medicinal Chemistry*, van de Waterbeemd, H., Testa,

B., and Folkers, G., Eds., Verlag Helvetica Chimica Acta, Basel, 1997, 367–378
12 El Tayar, N., Tsai, R.S., Testa, B., Carrupt, P.A., and Leo, A. Partitioning of solutes in different solvent systems: the contribution of hydrogen-bonding capacity and polarity. *J. Pharm. Sci.* 1991, **80**, 590–598
13 Abraham, M.H., Chadha, H.S., Whiting, G.S., and Mitchell, R.C. Hydrogen bonding. 32. An analysis of water–octanol and water–alkane partitioning and the δlog P parameter of Seiler. *J. Pharm. Sci.* 1994, **83**, 1085–1100
14 El Tayar, N., Testa, B., and Carrupt, P.A. Polar intermolecular interactions encoded in partition coefficients: an indirect estimation of hydrogen-bond parameters of polyfunctional solutes. *J. Phys. Chem.* 1992, **96**, 1455–1459.
15 Grid1.7 , 1999, Molecular Discovery Ltd, West Way House, Elms Parade, Oxford OX2 9LL
16 Sjöberg, P. MOLSURF - a generator of chemical descriptors for QSAR. In: *Computer-Assisted Lead Finding and Optimization. Current Tools for Medicinal Chemistry*, van de Waterbeemd, H., Testa, B., and Folkers, G., Eds., Wiley-VCH, Weinheim, 1997, 81–92
17 Norinder, U., Osterberg, T., and Artursson, P. Theoretical calculation and prediction of intestinal absorption of drugs in humans using MolSurf parametrization and PLS statistics. *Eur. J. Pharm. Sci.* 1999, **8**, 49–56
18 Palm, K., Artursson, P., and Luthman, K. Experimental and theoretical predictions of intestinal drug absorption. In: *Computer-Assisted Lead Finding and Optimization*, van de Waterbeemd, H., Testa, B., and Folkers, G., Eds., Wiley-VCH, Weinheim, 1997, 277–289
19 van de Waterbeemd, H., Camenisch, G., Folkers, G., Chrétien, J.R., and Raevsky, O.A. Estimation of blood–brain barrier crossing of drugs using molecular size and shape, and H-bonding descriptors. *J. Drug Targeting* 1998, **6**, 151–165
20 Palm, K., Stenberg, P., Luthman, K., and Artursson, P. Polar molecular surface properties predict the intestinal absorption of drugs in humans. *Pharm. Res.* 1997, **14**, 568–571
21 Gaillard, P., Carrupt, P.A., Testa, B., and Boudon, A. Molecular lipophilicity potential, a tool in 3D-QSAR. Method and applications. *J. Comput. -Aided Mol. Design* 1994, **8**, 83–96
22 Carrupt, P.A., Gaillard, P., Billois, F., Weber, P., Testa, B., Meyer, C., and Pérez, S. The molecular lipophilicity potential (MLP): a new tool for log P calculations and docking, and in comparative molecular field analysis (CoMFA). In: *Lipophilicity in Drug Action and Toxicology*, Pliska, V., Testa, B., and van de Waterbeemd, H., Eds., VCH Publishers, Weinheim, 1996, 195–217
23 Ash, S., Cline, M.A., Hower, R.W., Hurst, T., and Smith, G.B. Sybyl line notation (SLN). A versatile language for chemical structure representation. *J. Chem. Inf. Comput. Sci.* 1997, **37**, 71–79.
24 Pearlman, R.S., Balducci, R., Rusinko, A., Skell, J.M., and Smith, K.M. 1993, Tripos Associates, Inc., St-Louis, Missouri
25 Kamlet, M.J., Doherty, R.M., Abraham, M.H., Marcus, Y., and Taft, R.W. Linear solvation energy relationships. 46. An improved equation for correlation and prediction of octanol/water partition coefficients of organic nonelectrolytes (including strong hydrogen bond donor solutes). *J. Phys. Chem.* 1988, **92**, 5244–5255
26 Abraham, M.H. Scales of solute hydrogen-bonding: their construction and application to physicochemical and biochemical processes. *Chem. Soc. Rev.* 1993, 73–83
27 Taft, R.W., Abboud, J.L.M., Kamlet, M.J., and Abraham, M.H. Linear solvation energy relations. *J. Sol. Chem.* 1985, **14**, 153–186
28 Halgren, T.A. MMFF VII. Characterization of MMFF94, MMFF94s, and other widely available force fields for conformational energies and for intermolecular interaction energies and geometries. *J. Comput. Chem.* 1999, **20**, 730–748
29 Halgren, T.A. MMFF VI. MMFF94s option for energy minimization studies. *J. Comput. Chem.* 1999, **20**, 720–729
30 Andrews, P.R. Drug-receptor interactions. In: *3D QSAR in Drug Design. Theory Methods and Applications.*, Kubinyi, H., Ed., ESCOM Science Publishers, Leiden, 1993, 13–40
31 Andrews, P.R., and Tintelnot, M. Intermolecular forces and molecular binding. In: *Comprehensive Medicinal Chemistry. The Rational Design, Mechanistic Study & Therapeutic Applications of Chemical Compounds*, Ramsden, C.A., Hansch, C., Sammer, P.G., and Taylor, J.B., Eds., Pergamon, Oxford, 1990, 4, pp. 321–347
32 Vedani, A. and Dunitz, J. Lone-pair directionality in hydrogen bond potential functions for molecular mechanics calculations: the inhibition of human carbonic anhydrase II by sulfonamides. *J. Am. Chem. Soc.* 1985, **107**, 7653–7658
33 Gavezzotti, A. and Filippini, G. Geometry of the intermolecular X-H...Y (X,Y = N,O) hydrogen bond and the calibration of empirical hydrogen-bond potentials. *J. Phys. Chem.* 1994, **98**, 4831–4837
34 Boobbyer, D.N.A., Goodford, P.J., McWhinnie, P.M., and Wade, R.C. New hydrogen-bond potentials for use in determining energetically favorable binding sites on molecules of known structure. *J. Med. Chem.* 1989, **32**, 1083–1094
35 Bruno, I.J., Cole, J.C., Lommerse, J.P.M., Rowland, R.S., Taylor, R., and Verdonk, M.L. IsoStar: a library of information about nonbonded interactions. *J. Comput. -Aided Mol. Design* 1997, **11**, 525–537
36 Wahl, M.C., and Sundaralingam, M. C-H...O hydrogen bonding in biology. *TIBS* 1997, **22**, 97–102
37 Mills, J.E.J., and Dean, P.M. Three-dimensional hydrogen-bond geometry and probability information from a crystal survey. *J. Comput. -Aided Mol. Design* 1996, **10**, 607–622
38 Goodford, P.J. A computational proceudre for determining energetically favorable binding sites on biologically important macromolecules. *J. Med. Chem.* 1985, **28**, 849–857
39 Leahy, D.E., Morris, J.J., Taylor, P.J., and Wait, A.R. Model solvent systems for QSAR. Part 3. An LSER analysis of the "critical quartet". New light on hydrogen bond strength and directionality. *J. Chem. Soc. , Perkin Trans. 2* 1992, 705–722
40 Cruciani, G., Crivori, P., Carrupt, P.A., and Testa, B. Molecular fields in quantitative structure permeation relationships: the VolSurf approach. *J. Mol. Struct. (THEOCHEM)* 2000, **503**, 17–30
41 Cruciani, G., and Clementi, S. GOLPE: philosophy and

applications in 3D QSAR. In: *Advanced Computer-Assisted Techniques in Drug Discovery*, van de Waterbeemd, H., Ed., VCH Publishers, Weinheim, 1995, 61–88
42 Medchem, 1995, Daylight Chemical Information System, Inc., Irvine, California
43 Caron, G., Steyaert, G., Pagliara, A., Crivori, P., Gaillard, P., Carrupt, P.A., Avdeef, A., Box, K.J., Girault, H.H., and Testa, B. Structure–lipolicity relationships of the neutral and cationic forms of β-blockers. Part I. Partitioning in isotropic systems. *Helv. Chim. Acta* 1999, **82**, 1211–1222
44 Gaillard, P., Carrupt, P.A., and Testa, B. The conformational-dependent lipophilicity of morphine glucuronides as calculated from their molecular lipophilicity potential. *Bioorg. Med. Chem. Lett.* 1994, **4**, 737–742
45 Altomare, C., Cellamare, S., Carotti, A., Casini, G., Ferappi, M., Gavuzzo, E., Mazza, F., Carrupt, P.A., Gaillard, P., and Testa, B. X-ray crystal structure, partitioning behavior, and molecular modeling study of piracetam-type nootropics: insights into the pharmacophore. *J. Med. Chem.* 1995, **38**, 170–179
46 Caron, G., Gaillard, P., Carrupt, P.A., and Testa, B. Lipophilicity behavior of model and medicinal compounds containing a sulfide, sulfoxide, or sulfone moiety. *Helv. Chim. Acta* 1997, **80**, 449–462
47 Gavezzotti, A. The calculation of molecular volumes and the use of volume analysis in the investigation of structured media and of solid-state organic reactivity. *J. Am. Chem. Soc.* 1983, **105**, 5220–5225
48 Wade, R.C., Clark, K.J., and Goodford, P.J. Further development of hydrogen bond functions for use in determining energetically favorable binding sites on molecules of known structure. 1. Ligand probe groups with the ability to form two hydrogen bonds. *J. Med. Chem.* 1993, **36**, 140–147
49 Wade, R.C., and Goodford, P.J. Further development of hydrogen bond functions for use in determining energetically favorable binding sites on molecules of known structure. 2. Ligand probe groups with the ability to form more than two hydrogen bonds. *J. Med. Chem.* 1993, **36**, 148–156
50 Testa, B., and Kier, L.B. Complex systems in drug research. I. The chemical levels. *Complexity* 1996, **1**, 29–36
51 Kier, L.B., and Testa, B. Complex systems in drug research. II. The ligand-active site–water confluence as a complex system. *Complexity* 1996, **1**, 37–42
52 Testa, B., Kier, L.B., and Carrupt, P.A. A systems approach to molecular structure, intermolecular recognition, and emergence-dissolvence in medicinal research. *Med. Res. Rev.* 1997, **17**, 303–327
53 Testa, B., Carrupt, P.A., Gaillard, P., and Tsai, R.S. Intramolecular interactions encoded in lipophilicity: their nature and significance. In: *Lipophilicity in Drug Action and Toxicology*, Pliska, V., Testa, B., and van de Waterbeemd, H., Eds., VCH Publishers, Weinheim, 1996, 49–71
54 Lipinski, C.A., Lombardo, F., Dominy, B.W., and Feeney, P.J. Experimental and computational approaches to estimate solubility and permeability in drug discovery and development settings. *Adv. Drug Deliv. Rev.* 1997, **23**, 3–25